Nat Hazards (2011) 56:37–57
DOI 10.1007/s11069-010-9548-z

ORIGINAL PAPER

A new total volume model of debris flows with intermittent surges: based on the observations at Jiangjia Valley, southwest China

N. Sh. Chen · Ch. L. Yang · W. Zhou · F. Q. Wei · Z. L. Li · D. Han · G. Sh. Hu

Received: 28 October 2008 / Accepted: 22 April 2010 / Published online: 21 May 2010

Abstract Debris flow with intermittent surges is a major natural hazard. Accurate estimation of the total volume of debris flow is a challenge for academic researchers and engineering practitioners. This paper has proposed a new model for the total volume estimation based on 15 years of observations in Jiangjia Valley, China, from 1987 to 2004. The model uses two input variables: debris flow moving time and average surge peak discharge. The Weibull distribution formula is adopted to describe the relationship between the debris flow surge peak discharge and its relative frequency. By integrating the Weibull function and two-point curve fitting, the relationship between the maximum discharge and average surge peak discharge can be established. The total debris flow volume is linked with the debris flow moving time and the average peak discharge. With statistical regression, the debris flow moving time is derived from the debris flow total time. The proposed model has fitted very well with the validation data and outperformed the existing models. This study has provided a new and more accurate way for estimating the total volume of debris flows with intermittent surges in engineering practice.

Keywords Debris flow with intermittent surges · Total volume · Jiangjia Valley

N. Sh. Chen (✉) · Ch. L. Yang · W. Zhou · F. Q. Wei · Z. L. Li · G. Sh. Hu
Institute of Mountain Hazards and Environment, Chinese Academy of Sciences, 610041 Chengdu, People's Republic of China
e-mail: chennsh@imde.ac.cn

N. Sh. Chen · Ch. L. Yang · W. Zhou · F. Q. Wei · Z. L. Li · G. Sh. Hu
Mountain Hazard and the Earth's Surface Processes Key Laboratory, Chinese Academy of Sciences, 610041 Chengdu, People's Republic of China

Ch. L. Yang · W. Zhou · G. Sh. Hu
Graduate University of Chinese Academy of Sciences, 100093 Beijing, People's Republic of China

D. Han
Department of Civil Engineering, University of Bristol, Bristol, UK

1 Introduction

Debris flows are one of the most dangerous natural hazards, which can occur suddenly and destroy towns, highways, bridges etc. in a matter of minutes. Debris flows can be divided into two types, viscous and non-viscous debris flows. The bulk density of a viscous debris flow is usually above 1.8 g/cm^3 and that of a non-viscous debris flow is normally less than 1.8 g/cm^3. Non-viscous debris flows usually travel continuously from the beginning to the end, but viscous debris flows with a bulk density greater than 1.8 g/cm^3 tend to proceed in intermittent surges. It has been observed that viscous debris flows with intermittent surges are quite common and have caused many devastating disasters in the world. It has been reported that the most damaging intermittent debris flow disaster happened in the central downtown of Nianguaá in Venezuela during December 15–16, 1999, which led to at least 30,000 deaths and 100,000 people homeless (García-Martínez and López 2005; Francisco 2001). In China, intermittent debris flows are also widely distributed. For example, from June to August in 2003, there were ten disastrous debris flow events in southwest China with 144 people killed, among them eight were viscous debris flows with intermittent surges (Gerald and Nancy 2000).

To alleviate damages from debris flows, engineering measures such as trap dams and diversion channels have been widely used around the world. A key design parameter for these engineering structures is the total debris flow volume. Accurate estimation of this parameter is a challenging task, especially for those with intermittent surges. So far, there are still many problems with the existing volume estimation models, and this study was set to develop a new suitable model for debris flow volume with intermittent surges.

2 Background

2.1 Basic concept about debris flow with intermittent surges

Based on the long-period observation, we normally divide debris flows into continuous debris flow, intermittent debris flow with surges and hybrid debris flow (a mixture of both). It has been found that non-viscous debris flows usually move continuously, but viscous debris flows tend to move in intermittent surges or a hybrid state. Since intermittent debris flows are made of many individual surges, the total volume estimation of such debris flows is much harder to do than that of continuously debris flows.

2.1.1 The surge profile shape

An intermittent debris flow is composed of tens or hundreds of surges. A debris flow surge is divided into three parts: the front, tail and body. The three parts usually make the debris flow surge with a triangular profile shape (Matthias and Oldrich 2005) (Fig. 1). This triangular shape has been observed through the flow surface velocity, and it changes with flow thickness (Gerald and Nancy 2000).

2.1.2 The surge gap time and surge moving time

An intermittent debris flow moves with many surges. The time from a surge's initiation to stop is called the surge moving time (T_m). There is a quiet time between adjacent surges,

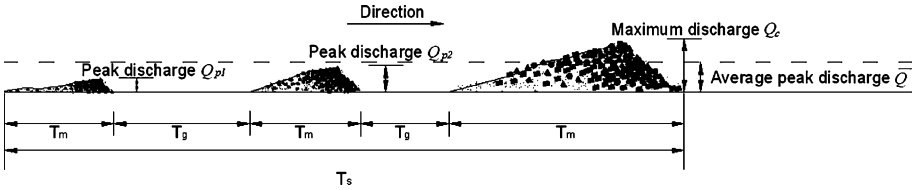

Fig. 1 The sketch map of debris flow surge processes

and it is called the surge gap time (T_g). During the surge gaps, no debris movement could be observed. The debris flow process time contains the surge moving time T_m and surge gap time T_g, therefore the process time for a surge $T = T_m + T_g$, and the total time for an intermittent debris flow $T_s = \sum (T_m + T_g) = T_M + T_G$.

2.1.3 The total volume

The total volume of a debris flow can be defined as all the liquefied geo-materials and water passing through a fixed cross-section perpendicular to the debris flow path. Similar to the total volume of water in a river, a debris flow total volume is a function of time and discharge. The peak discharge for each surge is a useful value for estimating the debris flow surge volume. The maximum discharge of a debris flow is defined as the largest peak discharge among all the surges.

2.1.4 The solid volume

A debris flow total volume includes both the solid material and water. The solid volume means the total amount of solid materials in a debris flow (excluding the water). The debris flow total volume M_c and debris flow solid volume W_c can be converted via the density relationship.

2.2 Empirical methods for debris flow volume

There are two main approaches for estimating the total debris flow volume: empirical methods and physics-based methods. Through literature review, we listed some typical empirical methods in Table 1. Models 1–2 in the table show that the debris flow total volume can be estimated by the maximum discharge and the process time. In the models 3–4, the debris flow solid material volume is linked to the maximum discharge of a debris flow.

2.3 Model simulation for debris flow volume

An alternative approach to empirical methods is physics-based model, such as the Newton fluid model and the two-phase debris flow model (Macro 1996; Takahashi and Tsujimoto 2000). By these models, the debris flow processes and the total volume could be obtained indirectly. Such a model has been applied in Nianguaá basin in Venezuela to simulate the debris flow processes of December 15–16, 1999.

Table 1 Some typical models for the solid material and total volume calculations

No.	Reference	Methods	Explanation	Notes
1	Ministry of Land and Resources (2006)	$M_c = KT_SQ_c$	M_c: The debris flow total volume T_S: The total process time of debris flow Q_c: The maximum discharge	K: F (catchment area) $F < 5$ km^2, $K = 0.202$ $F = 5$–10 km^2, $K = 0.113$ $F = 10$–100 km^2, $K = 0.0378$ $F > 100$ km^2, $K < 0.0252$
2	Zhou et al. (1991)	$M_c = 19T_SQ_c/72$	T_S: The total process time of debris flow Q_c: The maximum discharge M_c: The debris flow total volume	Pentagon calculation method
3	Costa (1988)	$Q_c = 0.293W_c^{0.56}$	W_c: The solid material volume Q_c: The maximum discharge	Indirect empirical method
4	Costa (1988)	$Q_c = 0.0163W_c^{0.64}$	W_c: The solid material volume Q_c: The maximum discharge	Indirect empirical method

2.4 Problems with the existing methods

Although some useful achievements have been made in the total volume estimation of debris flows, there are still many problems that need further research.

1. Many empirical methods are mostly relevant to a specific location. It is usually difficult to verify such empirical relations because they need a sufficient number of debris flows to occur at the same site; therefore, a long observation record is needed.
2. The physics-based model approach suffers from its difficulty in obtaining reliable model parameters either directly or indirectly. In addition, the model's accuracy is uncertain, and there is a lack of model validation. As a result, physics-based model is not widely used in practical engineering projects.
3. The debris flow maximum discharge and moving time have been widely used to estimate the total volume of a debris flow. However, it is not easy to find out the moving time due to the lack of observation at the project site.
4. The relationship between the maximum discharge and the average discharge and the relationship between the debris flow moving time and the total time have not been reliably established.

Therefore, there is an urgent need to build a new effective model to overcome the problems in the existing methods so that more accurate estimation for the total volume could be achieved for practical debris flow mitigation projects. However, it should be noted that the following difficulties in the model development have normally hampered many researchers to build and validate a reliable total volume model:

1. Only limited cases of the actual debris flows have been investigated and reported on their total volumes in the literature;

2. The direct observation of debris flow processes is usually very difficult, because they normally develop and finish very rapidly in mountainous areas;
3. The content, property and volume of a debris flow change with time during its movement (Pierson and Costa 1987; Hungr 1995). Therefore, the total volume of a debris flow is not easy to obtain;
4. In practice, most debris flow investigations could only provide the maximum discharge and total time, not the average discharge and debris flow moving time.

The long debris flow observation at Jiangjia Valley in China has provided us with useful comprehensive records in this study, which enabled us to overcome many of the aforementioned difficulties.

3 General framework

A general framework for the new model development is illustrated in Fig. 2. The key processes are: (1) The debris flow observation data in Jiangjia Valley of China between 1987 and 2004 were collected; (2) peak discharges of debris flow events were selected and the function between debris flow surge peak discharges and the relative frequency were built up; (3) On the basis of the function, the relationship between the total volume, the average peak discharge and debris flow moving time was established; (4) Build the relationship between the debris flow moving time and total time (this is because that in practical debris flow field work, we can only estimate the debris flow total time and the maximum discharge by measuring the mud line); (5) Validate the proposed model to show its effectiveness and errors; (6) Apply the model to debris flow total volume calculations in practice.

4 Observation site and data

Around the world, there are a few debris flow observation sites, such as St. Helen lahar (USA), Jinagjia valley (China), Shaoyue valley (Japan), Southern Italian (Zanchetta et al. 2002; You and Cheng 2005). Among them, the longest debris flow observation is in Jiangjia Valley and its data have been widely used in debris flow research, such as the case studies, debris flow impact force analysis, debris flow processes model, debris flow properties (Takahashi 1994; Cui 2005). Usually, there are more than ten debris flow events at the site every year, and they tend to last about 2–4 h each. Since 1987, modern ultrasonic devices for debris flow depth have been widely used in the observation to improve the measurement accuracy. The data have been collected at the Dongchuan Debris Flow Observation and Research Station. This station is a unique facility in the world with the longest and most complete record of debris flow processes (established since 1961). It is located in the lower reaches of Jiangjia Valley (103°08′E, 26°14′N), 30 km to Dongchuan and 190 km to Kunming. Further information on the station can be found at http://english.imde.cas.cn/fos/fs/dc/.

4.1 The overview of Jiangjia Valley

Jiangjia Valley lies between N 26°13′ to 26°17′ and E 103°06′ to 103°13′, which is on the right bank of the Xiaojiang River, a tributary of the Yangtse River. The drainage area

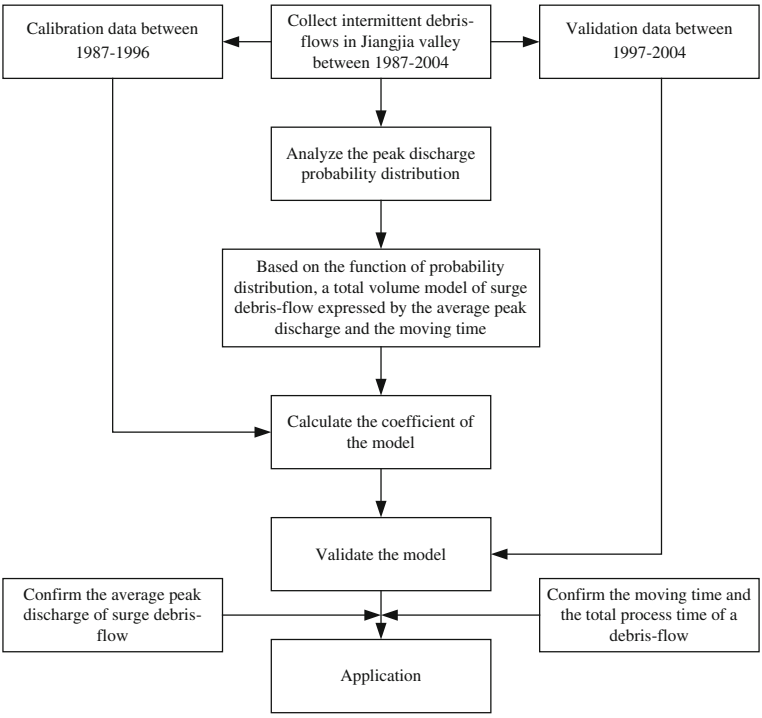

Fig. 2 The general flowchart of the model

of Jiangjia Valley is 48.6 km^2. The valley goes from the east to the west into the Xiaojiang River with a main channel of 13.9 km long and lies in a sub-tropical dry and hot area with a steep terrain. The bedrocks of the catchment are slate and schist of Precambrian, which have been highly weathered and weak in strength. The average annual precipitation of the area is about 700 mm. The annual evaporation varies between 1,700 and 3,700 mm. The precipitation in the summer between June and August takes up 80% of the whole year. The vegetation coverage rate of the catchment is less than 5%. Jiangjia Valley situates in the Xiaojiang fault and earthquake belt. During monsoon seasons, debris flows of different types happen frequently. In this study, we chose two sections with 200 m distance to observe debris flow's moving time and velocity (Figs. 3, 4).

4.2 Debris flow observation

Before each debris flow event, the width, depth and the cross-section area were measured. During the debris flow, an ultrasonic depth device UL-2 was used to check the debris flow depth (Fig. 4). The debris flow's front and its maximum depth were worked out from the difference between the surface and the channel bed. The peak discharge of a debris flow surge can be estimated on the basis of debris flow cross-section area and the average velocity. According to the triangular profile, the debris flow total volume can be calculated.

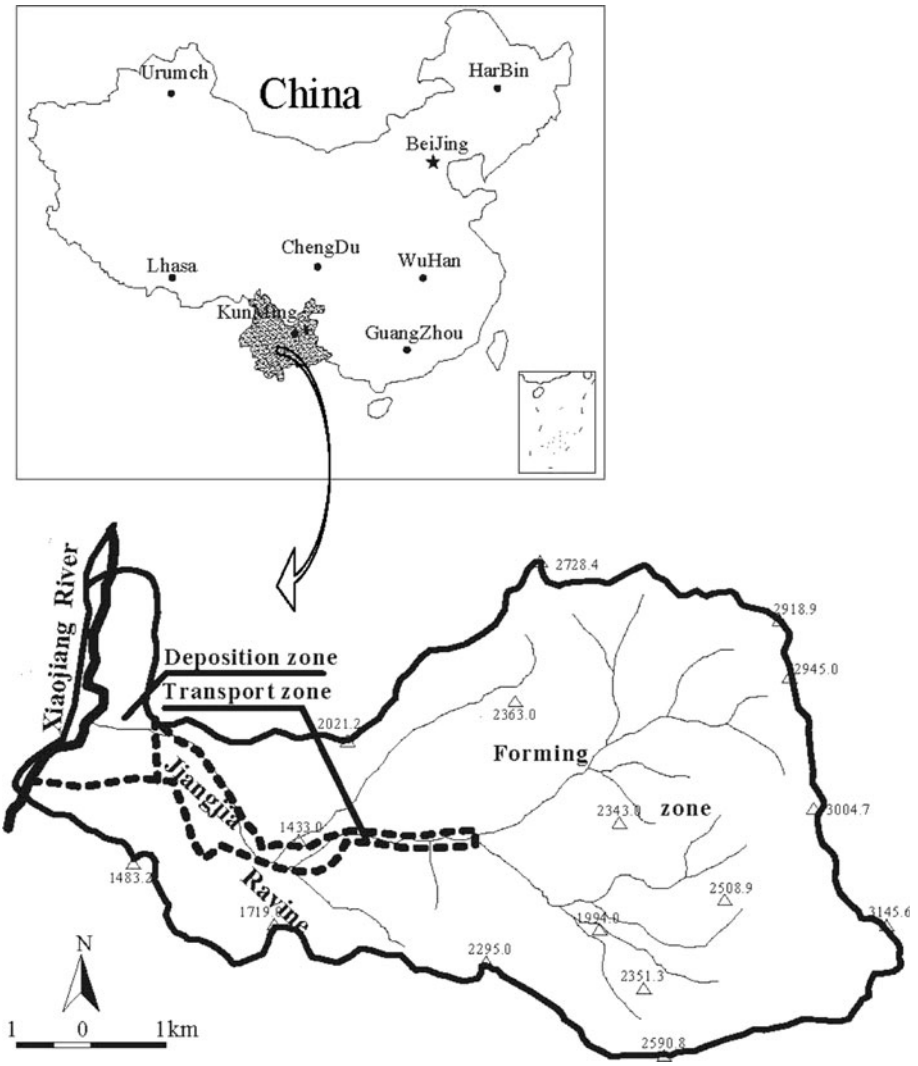

Fig. 3 Jiangjia Valley map

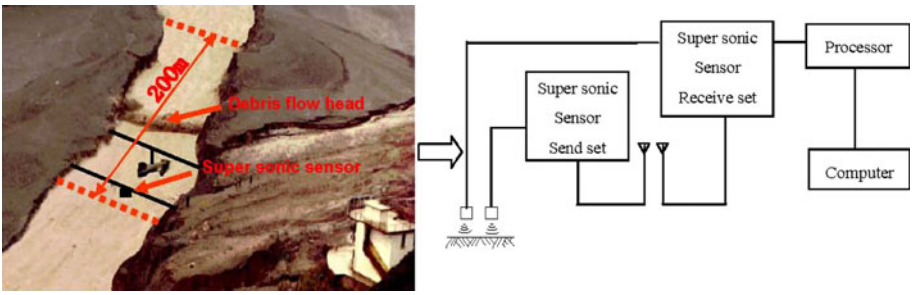

Fig. 4 The debris flow observation section and the flow chart of ultrasonic sensor system

4.3 Data selection

From 1987 to 2004, there were 128 intermittent debris flow recorded and there were 8,900 surges with these debris flows. On average, a debris flow lasts 4.2 h, varying between 0.7 and 16.4 h. There is a wide distribution of surge gap times. Take the debris flow of the No. 5 in 1989 as an example, we found the surge gap times were between 1 and 238 s and the average time is 65 s. An initial data analysis revealed that larger gaps between surges resulted in poor debris flow volume estimations. To derive a reliable statistical analysis, we limit the maximum surge gap time for each debris flow as 180 s (i.e., if a gap between two surges is greater than 180 s, the debris flow is divided into two different debris flows. They are called 'statistical' debris flows). Therefore, there were more 'statistical' debris flows than 128 as in the original data set. In addition, the minimum number of surges in a debris flow has been set to be greater than 15 (again, for statistical purposes). In this way, 151 'statistical' debris flows with 7,953 surges were chosen in this study. The duration for these debris flows varied between 0.3 and 9.3 h with an average duration of 1.1 h. The 151 debris flows were divided into two groups, of which 78 events in 1987–1994 were used to develop the model and the other 73 events in 1997–2004 were used for model validation and error analysis.

5 The total volume model

5.1 The distribution of surge peak discharges

A debris flow is composed of many surges, and there is a peak discharge for each surge. The debris flow peak discharges of surges are grouped according to their values. Histograms of surge peak discharges were developed for all the 78 debris flows in Table 2 with a bin size of 20 m^3/s. Two typical peak discharge distributions have been found, and they are illustrated in Fig. 5 based on Event No. 8806 and Event No. 8908-3. The curve type on the left represents 88% of the 78 debris flows and the one on the right represents 12%.

As the Weibull function is a widely used curve in environmental modeling(Sun 2001) and it is flexible to cope with both distributions in Fig. 5, we decided to use it to fit the surge peak discharge distributions. The Weibull probability density function is expressed as follows:

$$f(x) = crx^{r-1}\mathrm{e}^{-cx^r} \quad (x > 0) \tag{1}$$

The shape parameter $r > 0$, which controls the shape of the Weibull distribution curve; c is the scale parameter and shows the spread of the curve; x is the debris flow surge peak discharge (m^3/s). As illustrated in Fig. 5, the Weibull distribution can fit both histogram types reasonably well. In this study, no statistical test is performed on the curve fitting results. Traditionally, the chi-square test is used to work out the goodness of fit for curve fitting result. However, this is very subjective (i.e., the choice of statistical significance level) and controversial (from Bayesian statistics). The best way to avoid any subjectivity and controversy is to test the developed model with the validation data. If the new model can perform better with the validation data than the existing models, it is a good model. On the other hand, if the new model has a poorer validation result, it is a poor model regardless how well the peak discharge fits to a specific curve.

Table 2 Source data used in the model development

No.	Surges	Maximum discharge (m^3/s)	T_S (s)	T_M (s)	Median discharge (m^3/s)	The 3rd quartile discharge (m^3/s)
8703	23	254.0	2,149	1,144	101.70	157.50
8705	28	265.6	2,880	845	52.00	107.98
8707	53	795.4	4,571	2,610	288.00	430.30
8713	31	853.0	2,610	886	113.20	248.50
8715-1	16	412.7	1,280	454	98.50	280.95
8715-2	27	776.0	2,166	694	48.50	112.00
8715-3	44	728.9	4,128	1,382	56.15	106.65
8715-4	18	241.7	1,368	453	32.50	46.85
8715-5	20	264.0	1,555	528	65.65	90.48
8805-1	31	818.1	2,267	264	449.80	613.60
8805-2	22	692.1	1,772	321	84.10	206.15
8806	48	545.4	3,121	302	187.45	276.53
8808-1	75	613.6	5,279	708	70.00	101.78
8808-2	37	208.2	2,811	412	96.10	127.30
8905-1	22	1,029.0	2,173	720	222.95	556.23
8905-2	37	1,050.0	3,440	1,324	130.10	251.20
8905-3	55	515.3	5,480	1,986	97.50	200.10
8906	22	216.0	2,347	1,270	87.85	121.70
8907-1	21	740.9	1,712	975	340.90	591.55
8907-2	87	472.0	6,812	2,117	35.00	69.00
8908-1	32	220.0	3,001	1,136	76.95	107.10
8908-2	17	87.5	1,723	436	57.10	68.50
8908-3	21	56.8	2,297	710	30.80	39.25
8909	141	220.0	14,193	3,039	62.50	82.30
8911	107	240.0	7,936	3,127	101.40	153.80
8912	43	617.2	3,058	1,480	30.60	42.00
8914	35	81.8	3,270	2,260	45.00	45.00
9001	16	98.2	2,736	1,747	49.20	61.58
9003	85	467.8	8,605	5,523	72.20	130.45
9005	17	251.4	2,165	1,080	91.00	147.70
9006	63	285.3	6,909	4,249	61.50	100.50
9007	37	710.6	2,606	1,520	261.20	341.55
9008-1	46	518.6	4,571	2,655	135.20	180.50
9008-2	33	626.3	3,422	1,302	91.70	259.05
9009	38	660.2	3,443	1,735	252.60	455.80
9010	126	397.4	11,620	3,568	117.15	211.08
9101	41	376.5	3,547	1,152	90.90	199.00
9103	18	35.3	1,976	793	9.10	23.10
9105	168	754.0	18,980	11,113	151.95	292.73
9106	385	653.6	33,458	19,367	81.20	155.20
9108	204	648.7	21,228	13,686	201.80	371.25
9109-1	18	583.2	1,660	539	141.50	270.30
9109-2	16	193.0	1,545	524	81.55	126.68

Table 2 continued

No.	Surges	Maximum discharge (m^3/s)	T_S (s)	T_M (s)	Median discharge (m^3/s)	The 3rd quartile discharge (m^3/s)
9110-1	20	621.4	2,241	647	389.70	469.60
9110-2	48	546.8	3,966	2,007	103.60	204.88
9110-3	16	344.4	1,988	934	39.15	68.30
9111-1	16	674.4	1,575	737	209.60	383.38
9111-2	37	132.2	3,935	1,707	45.80	85.05
9112	29	267.1	3,492	1,206	79.90	151.00
9113	34	324.7	2,962	1,032	151.20	185.38
9114	94	452.2	9,162	4,793	169.65	227.68
9115	152	801.4	12,307	4,540	138.25	228.53
9116	175	545.5	14,999	6,622	136.50	207.30
9117-1	31	380.1	2,395	788	190.40	236.80
9117-2	19	611.1	1,567	488	257.70	400.50
9117-3	139	570.0	11,011	5,949	117.70	225.00
9118	83	589.0	9,830	6,511	79.60	231.20
9119	46	238.1	3,916	2,317	84.20	133.13
9122	17	151.2	1,160	338	42.40	79.95
9202	61	826.5	4,413	2,796	291.60	474.80
9203	21	308.4	2,744	1,130	95.20	191.00
9205-1	20	1,053.0	1,323	535	537.20	949.65
9205-2	27	767.3	3,345	993	183.50	326.10
9205-3	24	141.2	2,178	681	40.00	80.55
9206-1	47	746.6	4,088	1,984	277.40	420.00
9206-2	23	113.6	2,384	689	55.40	73.20
9301-1	19	481.9	1,803	876	180.40	282.00
9301-2	55	571.9	5,318	1,265	160.10	254.50
9301-3	23	139.0	1,611	307	22.10	43.70
9302-1	16	344.2	1,841	745	187.35	264.75
9302-2	30	364.9	2,652	817	81.00	125.73
9402-1	47	889.0	2,475	1,015	432.30	520.65
9402-2	71	805.5	7,091	3,436	100.85	280.85
9403-1	31	1,751.4	2,427	1,070	634.00	1,025.10
9403-2	29	436.3	2,773	875	105.80	296.20
9404-1	77	929.2	6,627	1,676	318.10	435.30
9404-2	35	261.1	2,203	467	37.60	64.70
9405	45	585.0	3,271	863	196.90	339.90

5.2 The total volume model

As seen in Fig. 1, each debris flow is composed of many surges with the triangular shape and the total volume can be derived as

$$M_c = \sum_{i=1}^{n} M_i = \frac{1}{2} \sum_{i=1}^{n} Q_i T_i \tag{2}$$

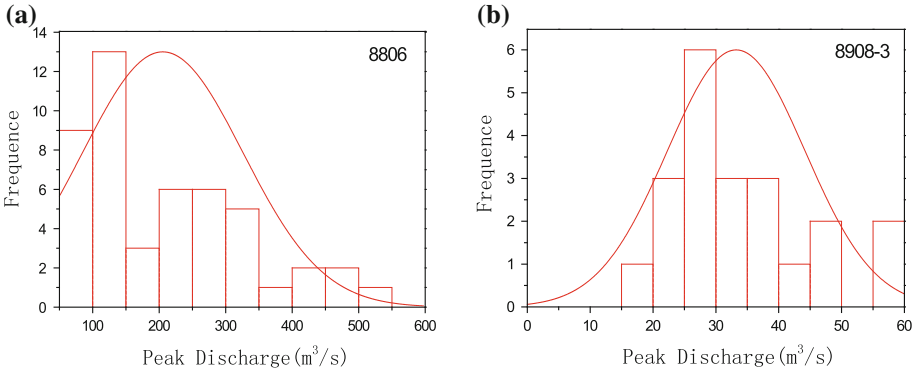

Fig. 5 The frequency curve of debris flow surge peak discharge

If an average surge peak discharge is known, the formula (2) can be simplified as

$$M_c = \frac{1}{2}\overline{Q}T_M \tag{3}$$

where M_c is the debris flow total volume, $\bar{Q}$ means the average surge peak discharge, T_M is the total debris flow surge moving time.

5.3 Average peak discharge calculation

From the Weibull distribution, the average surge peak discharge can be estimated from the expected value in the formula (1).

$$\overline{Q} = \int_0^{+\infty} xf(x)\mathrm{d}x = \frac{\Gamma(1+1/r)}{c^{1/r}} \tag{4}$$

in the formula (4) $\Gamma(r)$ is the Gamma function.

$$\Gamma(r) = \int_0^{+\infty} x^{r-1}\mathrm{e}^{-x}\mathrm{d}x \tag{5}$$

In order to calculate $\bar{Q}$, the parameters of c and r are to be decided. To work out these two parameters, a curve fitting can be carried out by plotting the measured data points in a frequency graph. As the Weibull distribution model contains two parameters, it is reasonable to choose two points in the plot, at $Q_{1/2}$ and $Q_{3/4}$. Although more accurate estimation by the least square method is possible, we decided to use the two-point method to simplify the computation process.

Suppose a debris flow event consists of n surges, the derivation of the two points can be carried out as:

1. $Q_{1/2}$ Algorithm: Sort the surges by the peak discharge in an ascending order.

   If n is odd, then $Q_{1/2} = Q_{(n+1)/2}$
   If n is even, then $Q_{1/2} = \left(Q_{n/2} + Q_{n/2+1}\right)/2$

2. $Q_{3/4}$ Algorithm: Sort the surges by the peak discharge in an ascending order.

If $3(n+1)/4$ is an integer, then $Q_{3/4} = Q_{3(n+1)/4}$
If $3(n+1)/4$ is not an integer, then

$$Q_{3/4} = Q_{[3(n+1)/4]} + \left(Q_{[3(n+1)/4]+1} - Q_{[3(n+1)/4]}\right) \times (3(n+1)/4 - [3(n+1)/4])$$

(Note: the notation [] represents the rounded part of a number, for instance: [5.3] = 5)

On the basis of the Weibull probability function integration, the distribution function can be obtained as:

$$F(x) = \int_0^x f(x)\mathrm{d}x = \int_0^x crx^{r-1}\mathrm{e}^{-cx^r}\mathrm{d}x = 1 - \mathrm{e}^{-cx^r} \tag{6}$$

Set it to 1/2 and 3/4:

$$1 - \mathrm{e}^{-cQ_{1/2}^r} = 1/2 \tag{7}$$

$$1 - \mathrm{e}^{-cQ_{3/4}^r} = 3/4 \tag{8}$$

Combining formulae (7) and (8), the parameter c and r are written as:

$$r = \frac{\ln\frac{1}{2}}{\ln\left(\frac{Q_{1/2}}{Q_{3/4}}\right)} \tag{9}$$

$$c = \frac{-\ln\left(\frac{1}{2}\right)}{Q_{1/2}^r} \tag{10}$$

Therefore, it is feasible to calculate the parameters of c and r via the median and 3rd quartile peak discharge. The reason to choose both points $Q_{1/2}$ and $Q_{3/4}$ is that these two discharge points are steadier comparing to other discharge points. Table 2 lists the maximum, median and 3rd quartile discharge from 1987 to 1994 debris flow records. From this table, we can plot the relationship between the maximum discharge, median and 3/4 surge peak discharges as shown in Figs. 6 and 7.

Linear regressions can be used to link the maximum discharge with the median and 3/4 surge peak discharges as

$$Q_{1/2} = k_1 Q_{\max} + b_1 \tag{11}$$

$$Q_{3/4} = k_2 Q_{\max} + b_2 \tag{12}$$

The parameters can be derived from the observed data, and the fitted regression equations are

$$Q_{1/2} = 0.3Q_{\max} - 6 \quad R^2 = 0.542 \tag{13}$$

$$Q_{3/4} = 0.5Q_{\max} - 16 \quad R^2 = 0.650 \tag{14}$$

5.4 The surge moving time T_M

The total debris flow time is relatively easier to obtain than the total surge moving time. From the observed total debris flow time T_S and moving surge time T_M (1987–1994), the scatter plot can be constructed as in Fig. 8. Clearly, there is a non-linear relationship between these two variables. A curve can be fitted to this plot as:

$$T_M = 0.1088 \times T_S^{1.1502} \quad R^2 = 0.8157 \tag{15}$$

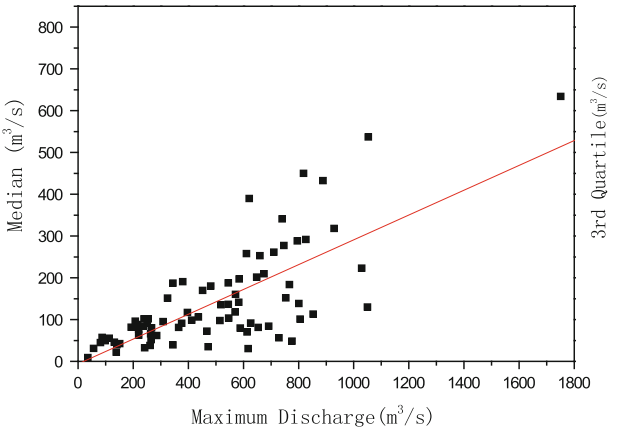

Fig. 6 The maximum discharge and median surge peak discharge

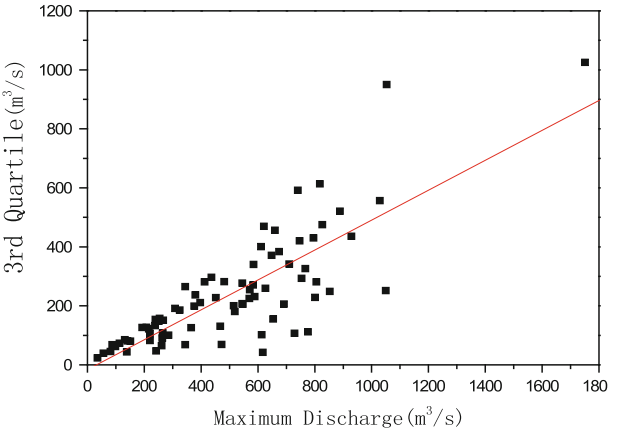

Fig. 7 The maximum discharge and 3rd quartile surge peak discharge

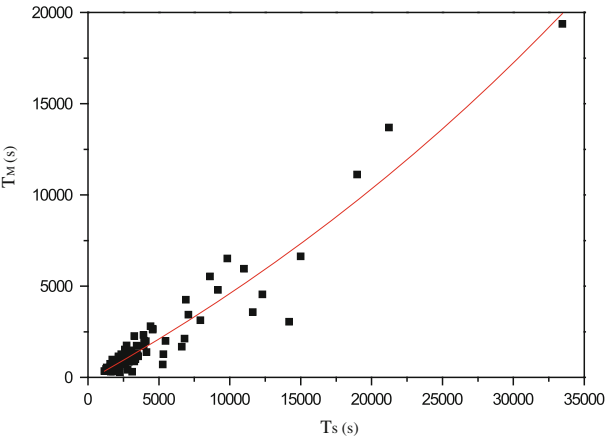

Fig. 8 The total time and moving time of debris flows

Formula (15) is very useful for deriving the total surge moving time from the total debris flow time; therefore, it has a practical usage in debris flow engineering designs.

6 Model validation

The newly developed volume model is validated with the observed data from 1997 to 2004. In addition, comparisons have been made with the existing models. To save space, only the results from the pentagon model and Crosta's first model are presented here (the performances from the other two models are at the similar level): $Q_c = 0.293W_c^{0.56}$ (Table 1). A density conversion was made to convert the solid volume to the total volume in Crosta's model. The results are listed in Table 3 and illustrated in Fig. 9. It has been found that the total volume calculated from the proposed model is very close to the observed data, but both Crosta's first model and the pentagon model are far away from the measurements. The error of the proposed model means: $E_{pr} = (Q_{pr} - Q_A)/Q_A \cdot 100\%$.

7 Discussion

The model validation has demonstrated that the proposed model worked very well and had a much better performance than the other two existing models. The average relative error of the proposed model is 40.5% and that of the pentagon model and Crosta's model are 475.6, 2,202.5%, respectively (Table 3). The reason underlining Crosta's model's poor results is likely that the model only uses the maximum discharge to get the debris flow total volume, without considering the effect of the total time. This would cause large errors in the result of debris flow with intermittent surges. The pentagon model performed much better than Crosta's, but its error is still too large for practical engineering projects. The proposed model is a huge improvement over the existing models. However, there are still many uncertain issues with the proposed model, and more research is still needed to address the following error sources: (1) the processes of debris flows with intermittent surges are very complicated, but only two parameters (average peak discharge and debris flow duration) have been taken into account in this study; (2) there is still a large uncertainty in the relationship between the debris flow total time and total debris flow moving time; (3) the maximum discharge is assumed in proportion to the total volume but in reality, this relationship may change with different debris flow characteristics; (4) although the Weibull distribution is used in this study, other probability distributions should be explored to see whether further improvements could be made; (5) the superior performance from the newly developed model may be attributed to the locally calibrated parameters and the model's generality is not proved in this study. The proposed model should be applied to other debris flow sites to test its general applicability. A good performance at Jianjia Valley site may not be replicated at other places.

To apply the proposed model in engineering practice, two basic parameters are to be estimated: the average peak discharge $\bar{Q}$ and debris flow moving time T_M. From the regression analysis, these two parameters can be derived from the maximum discharge and the debris flow time T_S. The practical method for maximum discharge estimation is to measure the mud-line sections and estimate the velocity (Chen et al. 2006). For example, Johnson and Rodine (1984), Rickenmann and Zimmermann (1993) and Crosta (2001) estimated maximum discharges for several debris flow sites based on field measurements of mud-line height and empirical equations such as the Manning–Sticker equation and the

Table 3 Source data used to validate and error analyze

No.	T_S (s)	Maximum discharge (m^3/s)	Q_A: Actual discharge (m^3/s)	$\overline{Q}$ (m^3/s)	T_M (s)	Q_{pr}: The proposed model (m^3/s)	E_{pr}: Error of the proposed model (%)	Q_{pa}: Pentagon model (m^3/s)	E_{pa}: Error of Pentagon model (%)	Q_{co}: Crosta's model (m^3/s)	E_{co}: Error of Crosta's model (%)
9705-1	1,322	1332.8	73,496	468.6	423	99,109.0	34.8	464,962.1	532.6	5,616,212.4	7,541.5
9705-2	1819	942.5	32,717	328.6	611	100,452.0	207.0	452,413.1	1,282.8	3,024,981.8	9,145.9
9705-3	2,795	709.0	44,190	244.3	1,002	122,295.5	176.7	522,936.7	1,083.4	1,819,473.6	4,017.4
9705-4	5,391	261.0	74,820	83.1	2,132	88,628.3	18.5	371,305.1	396.3	305,446.8	308.2
9705-5	2,091	516.0	54,088	174.9	717	62,672.9	15.9	284,724.5	426.4	1,031,628.6	1,807.3
9705-6	3,794	360.0	72,300	118.9	1,423	84,597.7	17.0	360,430.0	398.5	542,415.3	650.2
9705-7	1,824	174.0	20,110	52.0	613	15,912.7	−20.9	83,752.0	316.5	148,076.7	636.3
9706-1	4,624	856.8	155,093	297.9	1,787	266,074.7	71.6	1,045,486.0	574.1	2,551,471.9	1,545.1
9706-2	2,911	642.6	95,451	220.5	1,049	115,686.2	21.2	493,632.8	417.2	1,526,461.7	1,499.2
9708	7,140	899.9	476,549	313.3	2,945	461,362.9	−3.2	1,695,562.0	255.8	2,785,177.8	484.4
9709	1,132	1,005.8	75,921	351.3	354	62,108.7	−18.2	300,454.8	295.7	3,397,300.5	4,374.8
9710-1	5,372	971.0	375,935	338.8	2,123	359,741.7	−4.3	1,376,500.0	266.2	3,190,260.2	748.6
9710-2	1,356	399.8	21,646	133.1	436	28,988.9	33.9	143,061.8	560.9	654,114.7	2,921.9
9711-1	3,329	643.8	144,509	225.1	1,225	137,786.5	−4.7	565,569.4	291.4	1,531,555.7	959.8
9711-2	2,060	310.5	32,180	101.0	705	35,603.8	10.6	168,791.3	424.5	416,501.0	1,194.3
9711-3	3,982	1,282.5	272,273	450.5	1,505	339,035.9	24.5	1,347,658.0	395.0	5,243,345.8	1,825.8
9711-4	2,556	327.2	75,138	107.0	904	48,334.1	−35.7	220,696.4	193.7	457,345.2	508.7
9712	1,115	227.7	11,511	71.2	348	12,389.5	7.6	66,997.6	482.0	239,377.3	1,979.6
9713	3,914	699.9	203,468	241.0	1,475	177,751.1	−12.6	722,899.5	255.3	1,777,982.4	773.8
9714	2,735	699.7	218,391	241.0	977	117,727.1	−46.1	504,998.8	131.2	1,777,075.3	713.7
9715-1	2,983	658.6	217,902	226.3	1,079	122,067.7	−44.0	518,437.1	137.9	1,594,994.3	632.0
9715-2	2,630	400.1	81,573	133.2	934	62,216.1	−23.7	277,680.5	240.4	654,991.1	703.0
9716	2,074	336.0	18,230	110.1	711	39,119.7	114.6	183,894.7	908.7	479,541.5	2,530.5

Table 3 continued

No.	T_S (s)	Maximum discharge (m^3/s)	Q_A: Actual discharge (m^3/s)	$\overline{Q}$ (m^3/s)	T_M (s)	Q_{pr}: The proposed model (m^3/s)	E_{pr}: Error of the proposed model (%)	Q_{pa}: Pentagon model (m^3/s)	E_{pa}: Error of Pentagon model (%)	Q_{co}: Crosta's model (m^3/s)	E_{co}: Error of Crosta's model (%)
9717-1	1,571	770.0	109,733	266.1	516	68,762.1	−37.3	319,218.5	190.9	2,108,403.7	1,821.4
9717-2	3,810	589.7	109,291	201.6	1,430	144,187.2	31.9	592,894.2	442.5	1,309,367.7	1,098.1
9801	2,102	2,508.8	367,583	892.4	722	322,212.1	−12.3	1,391,617.0	278.6	17,377,253.0	4,627.4
9803	2,169	661.8	50,322	227.4	748	85,035.1	69.0	378,797.8	652.7	1,608,859.5	3,097.1
9804	2,707	945.0	104,777	329.5	965	158,962.1	51.7	675,058.1	544.3	3,039,325.0	2,800.8
9808	1,718	1,026.6	76,210	358.8	572	102,666.8	34.7	465,420.5	510.7	3,523,776.1	4,523.8
9809	2,182	1,680.0	292,960	594.5	753	223,789.0	−23.6	967,353.3	230.2	8,491,548.8	2,798.5
9901	2,149	1,123.6	128,834	393.5	740	145,596.7	13.0	637,190.4	394.6	4,140,254.1	3,113.6
9903-1	1,535	908.2	78,534	316.3	503	79,565.9	1.3	367,884.1	368.4	2,831,216.0	3,505.1
9903-2	1,590	241.7	12,261	76.3	523	19,965.6	62.8	101,413.3	727.1	266,291.4	2,071.9
9905	5,151	756.8	139,531	261.4	2,023	264,391.8	89.5	1,028,712.0	637.3	2,044,296.0	1,365.1
9906-1	3,325	924.4	207,452	322.1	1,223	196,901.1	−5.1	811,096.8	291.0	2,922,028.9	1,308.5
9906-2	1,759	689.0	67,374	237.1	588	69,769.0	3.6	319,820.4	374.7	1,728,839.4	2,466.0
9906-3	3,641	331.6	63,957	108.6	1,358	73,669.1	15.2	318,607.7	398.2	468,385.5	632.3
9907-1	1,287	613.9	44,939	210.3	410	43,170.5	−3.9	208,495.8	364.0	1,406,863.1	3,030.6
9907-2	1,831	299.6	31,208	97.0	616	29,845.8	−4.4	144,760.9	363.9	390,752.8	1,152.1
9907-3	1,635	181.2	19,293	54.6	541	14,749.1	−23.6	78,180.3	305.2	159,195.7	725.1
9908-1	2,218	1,063.8	121,641	372.1	768	142,782.6	17.4	622,648.1	411.9	3,755,027.9	2,987.0
9908-2	2,478	1,350.0	106,966	474.8	872	207,094.8	93.6	882,787.5	725.3	5,746,293.2	5,272.1
9909-1	4,496	1,118.9	224,177	391.9	1,730	339,047.1	51.2	1,327,513.0	492.2	4,109,378.9	1,733.1
9909-2	4,476	736.3	70,882	254.1	1,721	218,653.5	208.5	869,693.0	1,127.0	1,946,465.7	2,646.1
9909-3	2,855	335.3	27,176	109.9	1,026	56,382.5	107.5	252,616.0	829.6	477,758.9	1,658.0
2002	2,043	693.4	81,701	238.7	698	83,351.2	2.0	373,829.3	357.6	1,748,604.0	2,040.2

Table 3 continued

No.	T_S (s)	Maximum discharge (m^3/s)	Q_A: Actual discharge (m^3/s)	$\overline{Q}$ (m^3/s)	T_M (s)	Q_{pr}: The proposed model (m^3/s)	E_{pr}: Error of the proposed model (%)	Q_{pa}: Pentagon model (m^3/s)	E_{pa}: Error of Pentagon model (%)	Q_{co}: Crosta's model (m^3/s)	E_{co}: Error of Crosta's model (%)
2003	4,964	441.3	78,190	148.2	1,939	143,624.4	83.7	578,078.5	639.3	780,270.5	897.9
2004	1,782	553.7	42,634	188.3	597	56,173.9	31.8	260,377.4	510.7	1,170,066.5	2,644.4
2007-1	1,280	1,133.1	61,783	397.0	408	80,970.2	31.1	382,736.0	519.5	4,202,971.8	6,702.8
2007-2	2,149	465.4	35,306	156.8	740	58,003.0	64.3	263,927.0	647.5	857,989.0	2,330.2
2103	1,653	454.9	29,674	153.0	547	41,890.2	41.2	198,431.2	568.7	823,729.3	2,675.9
2109	3,220	326.8	33,813	106.8	1,179	62,982.4	86.3	277,689.2	721.2	456,347.2	1,249.6
2110	1,853	277.8	27,640	89.3	624	27,837.7	0.7	135,840.3	391.5	341,439.4	1,135.3
2113	2,867	747.0	148,883	257.9	1,031	132,922.9	−10.7	565,157.4	279.6	1,997,265.0	1,241.5
2114	1,508	180.9	11,011	54.5	493	13,423.1	21.9	71,988.15	553.8	158,725.4	1,341.5
2115-1	4,238	755.8	121,378	261.1	1,617	210,998.4	73.8	845,257.3	596.4	2,039,474.8	1,580.3
2115-2	2,241	454.7	47,938	153.0	777	59,422.6	24.0	268,898.2	460.9	823,082.7	1,617.0
2115-3	3,969	938.9	205,973	327.3	1,499	245,361.8	19.1	983,380.4	377.4	3,004,380.1	1,358.6
2116	4,949	780.6	160,729	269.9	1,932	260,837.7	62.3	1,019,453.0	534.3	2,160,513.7	1,244.2
2117-1	1,742	374.4	28,423	124.0	581	36,047.8	26.8	172,109.6	505.5	581,766.4	1,946.8
2117-2	2,645	1,110.1	166,598	388.7	940	182,737.8	9.7	774,834.4	365.1	4,051,843.5	2,332.1
2203	3,466	286.6	33,013	92.4	1,283	59,233.7	79.4	262,135.5	694.0	360,993.4	993.5
2204-1	1,843	629.8	59,260	216.0	620	66,995.4	13.1	306,301.5	416.9	1,472,591.3	2,385.0
2204-2	1,988	359.5	57,198	118.7	677	40,184.8	−29.7	188,597.7	229.7	541,070.8	846.0
2205	6,162	641.3	196,102	220.1	2,486	273,601.3	39.5	1,042,807.0	431.8	1,520,951.6	675.6
2207-1	1,641	557.5	67,014	189.7	543	51,454.3	−23.2	241,420.7	260.3	1,184,444.6	1,667.5
2207-2	3,677	863.2	156,478	300.1	1,373	206,104.3	31.7	837,579.7	435.3	2,585,605.0	1,552.4
2209	1,783	704.2	51,934	242.6	597	72,459.6	39.5	331,335.9	538.0	1,797,535.7	3,361.2
2302	2,327	1,322.8	134,684	465.0	811	188,608.7	40.0	812,291.1	503.1	5,541,187.1	4,014.2

Table 3 continued

No.	T_S (s)	Maximum discharge (m^3/s)	Q_A: Actual discharge (m^3/s)	$\overline{Q}$ (m^3/s)	T_M (s)	Q_{pr}: The proposed model (m^3/s)	E_{pr}: Error of the proposed model (%)	Q_{pa}: Pentagon model (m^3/s)	E_{pa}: Error of Pentagon model (%)	Q_{co}: Crosta's model (m^3/s)	E_{co}: Error of Crosta's model (%)
2306	1,994	1,103.8	88,800	386.4	679	131,210.5	47.8	580,813.4	554.1	4,010,872.8	4,416.7
2405	1,199	140.9	5,648	40.1	378	7,594.0	34.5	44,581.2	689.3	101,589.1	1,698.7
2407-1	2,252	840.0	73,634	291.8	781	114,005.7	54.8	499,193.3	577.9	2,462,823.8	3,244.7
2407-2	1,346	261.7	17,480	83.4	432	18,032.3	3.2	92,954.4	431.8	306,911.2	1,655.8

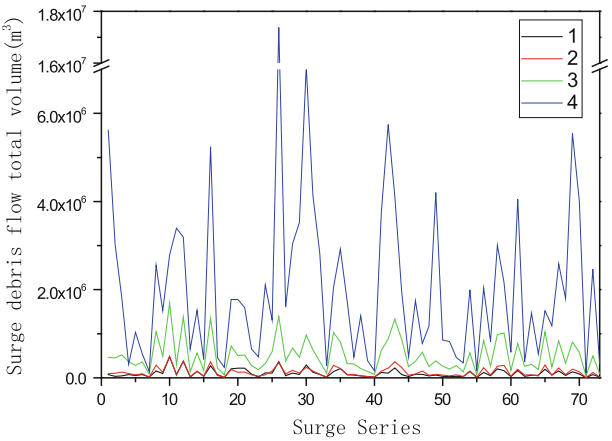

Fig. 9 The compare picture of three methods results and practice observation value *1* observed data, *2* the proposed model, *3* pentagon model, *4* Crosta's model

Chézy equation. Besides, on the basis of flood discharge and its possibly relative debris load, the debris flow maximum discharge can also be estimated (Du 1986; Zhong 2002). In addition, Dunne (1987) and Whipple (1992) calculated the maximum discharge of a debris flow based on the amount and stability of the source materials. Chen (2001) proposed to estimate the maximum discharges of debris flows with various frequencies using runoff and precipitation records, equivalent flow duration contours in small basins and the ratio of soil particles to water estimated from the sedimentary structure of debris flow deposits. Zanchetta et al. (2002) developed empirical equations concerning debris flow volume and maximum discharge and applied them to a volcaniclastic debris flow in the Sarno area, southern Italy. Hungr et al. (1984), Rickenmann (1999), Matthias and Oldrich (2005) also developed numerical models to calculate the maximum discharge of a debris flow from empirical equations. Similar hydrological approaches were also taken by Macro (1996) as well as by He and Chen (2001). Therefore, the maximum discharge of debris flow can be obtained by many alternative approaches.

The debris flow total time can be estimated by the report from eye witnesses, which is used widely in populous China. Besides, it also can be checked by the recorder of rain gauges or weather radars. It is revealed that the triggering of most debris flow is due to heavy rains, of which the intensity is beyond the precipitation threshold. The debris flow processes usually accord with the raining processes well (Laurence and Greg 1994). Usually, the apex of debris flow maximum discharge is the same with the peaking raining time (Takahashi 1994). Therefore, the total time of debris flow processes can be estimated by the rainfall record analysis. In this study, the recorded debris peak discharges and flow moving times have been used in model validation and model comparison. This study did not carry out the comparison between different estimation methods for debris flow peak discharges and moving times, which should be a future study area.

8 Conclusion

The debris flow total volume is an important parameter for debris flow mitigation and research. Based on the debris observation in Jiangjia Valley from 1987 to 2004, a new total

volume calculation model has been developed and validated. The model uses two input variables: debris flow moving time and average surge peak discharge. The Weibull distribution formula is adopted to describe the relationship between the debris flow surge peak discharge and the relative frequency. By integrating the Weibull function and two-point curve fitting, the relationship between the maximum discharge and average surge peak discharge can be established. The total debris flow volume is linked with the debris flow moving time and the average peak discharge. With statistical regression, the debris flow moving time is derived from the debris flow total time. The proposed model has fitted very well with the validation data and outperformed the existing models. This study has provided a new way for estimating the total volumes of debris flows with intermittent surges in engineering practice, and it should also stimulate further research activities in this field to search for more accurate methods.

Acknowledgments The authors would like to thank the financial supports from the Scholarship of Knowledge Innovation Project, Chinese Academy of Sciences (KZCX2-YW-332) and the Western Talent Grants of Chinese Academy of Sciences. The authors are grateful for the valuable comments and suggestions from Professor Tian Lianquan which improved the quality of the paper. The observation data had been recorded by Dongchuan debris flow observation and research station, Chinese Academy of Sciences. At the same time, the authors would like to express our heartfelt gratitude to the reviewers and editors who brought forward valuable suggestions and helped us improve the contents and presentation of the manuscript.

References

Chen NS (2001) The research on gravity viscous debris flow in flow confluence in small basin. J Mt Sci 19:418–424 (in Chinese)

Chen NS, Yue ZQ, Cui P, Li ZL (2006) A rational method for estimating maximum discharge of a landslide-induced debris flow: a case study from southwestern China. Geomorphology 84:44–58

Costa JE (1988) Floods from dam failures. In: Baker VR et al (eds) Flood geomorphology. Wiley, New York, pp 439–463

Crosta GB (2001) Failure and flow development of a complex slide: the 1993 Sesa landslide. Eng Geol 59:173–199

Cui P (2005) The forecasting of debris flow. Bull Chin Acad Sci 5:363–369 (in Chinese)

Du RH (1986) The advances on debris flow research in China. J Mt Res 4:70–73 (in Chinese)

Dunne T (1987) Sediment routing by debris flow. In: Bestcha RL, Blinn T, Grant GE, Ice GG, and Swanson FJ (eds) Process erosion and sedimentation in Pacific Rim, vol 165. JAHS Publication, pp 213–223

Francisco LP (2001) Matrix granulometry of catastrophic debris flows (December 1999) in central coastal, Venezuela. CATENA 45:163–183

García-Martínez R, López JL (2005) Debris flow of December 1999 in Venezuela. In: Jakob M, Hungr O (eds) Debris flows hazards and related phenomena. Praxis Publishing Ltd, Chichester, pp 519–538

Gerald FW, Nancy DN (2000) Debris-flow hazards mitigation: mechanics, prediction, and assessment. Balkema, Rotterdam, pp 255–262

He J, Chen NS (2001) Application of debris flow overstep in curve ways to velocity calculation. J Chengdu Univ Technol 28:425–428 (in Chinese)

Hungr O (1995) A model for the runout analysis of rapid flow slides. Can Geotech J 32:610–623

Hungr O, Morgan GC, Kellerhals R (1984) Quantitative analysis of debris torrent hazard for design of remedial measures. Can Geotech J 21:663–677

Johnson AM, Rodine JR (1984) Debris flow. In: Brunsden D, Prior DB (eds) Slope instability, Chapter 8. Wiley, Chichester, pp 257–357

Laurence CS, Greg AO (1994) Within-storm variations in runoff and sediment export from a rapidly eroding coal-refuse deposit. Short Communication 370–375

Macro F (1996) Use of a genetic algorithm combined with a local search method for the automatic calibration conceptual rainfall-runoff model. Hydrol Sci J 41:21–39

Matthias J, Oldrich H (2005) Debris flows hazards and related phenomena. Praxis Publishing Ltd, Chichester, pp 15–20

Ministry of Land and Resources (2006) Specification of geological investigation for debris flow stabilization, China. Ministry of land and resources of the People's Republic of China, pp 27 (in Chinese)
Pierson TC, Costa JE (1987) A rheologic classification of subaerial sediment-water flows. In: Costa JE, Wieczorek GF (eds) Debris flows/avalanches: process, recognition and mitigation. Geol Soc Am Rev Eng Geol, vol 7, pp 1–12
Rickenmann D (1999) Empirical relationships for debris flows. Nat Hazards 19:47–77
Rickenmann D, Zimmermann M (1993) The 1987 debris flow in Switzerland: documentation and analysis. Geomorphology 8:175–189
Sun DH (2001) Mathematic method and application of sediment granularity classification of the ancient environment. Dev Nat Sci 3:269–276 (in Chinese)
Takahashi T (1994) Japan–China joint research on the prevention from debris flow hazards. Research report of the grant-in-aid for scientific research. pp 56–58
Takahashi T, Tsujimoto H (2000) A mechanical model for Merapi-type pyroclastic flow. J Volcanol Geotherm Res 98:91–115
Whipple KX (1992) Predicting debris flow run out and deposit on fans: the importance of the flow hydrograph. In: Walling DE, Davis TR, Hasholt B (eds) Debris flows and environment in mountain regions. IAHS publication no. 209. Wallingford, UK, pp 337–345
You Y, Cheng ZL (2005) The influence of discontinuous motion of viscous debris flow on erosion and deposition of gully bed—study of the case at Jiangjia gully in Dongchuan, Yunnan. J Disaster Prev Mitig Eng 6:47–149 (in Chinese)
Zanchetta G, Sulpizio R, Pareschi MT, Leoni FM, Santacroce R (2002) Characteristics of May 5–6, 1998 volcaniclastic debris flows in the Sarna area (Campania, southern Italy): relationships to structural damage and hazard zonation. J Volcanol Geotherm Res 133:377–393
Zhong DL (2002) Field survey for debris flow. Bull Soil Water Conserv 12:59–61 (in Chinese)
Zhou BF, Li DJ et al (1991) The directory of debris flow prevention and control. Science Press, China, p 92 (in Chinese)